Functional selection of protease inhibitory antibodies

Tyler Lopez[a], Zahid Mustafa[a], Chuan Chen[a], Ki Baek Lee[a], Aaron Ramirez[a], Chris Benitez[a], Xin Luo[b], Ru-Rong Ji[b], and Xin Ge[a,1]

[a]Department of Chemical and Environmental Engineering, University of California, Riverside, CA 92521; and [b]Center for Translational Pain Medicine, Department of Anesthesiology, Duke University Medical Center, Durham, NC 27710

Edited by James A. Wells, University of California, San Francisco, CA, and approved July 8, 2019 (received for review February 25, 2019)

Critical for diverse biological processes, proteases represent one of the largest families of pharmaceutical targets. To inhibit pathogenic proteases with desired selectivity, monoclonal antibodies (mAbs) hold great promise as research tools and therapeutic agents. However, identification of mAbs with inhibitory functions is challenging because current antibody discovery methods rely on binding rather than inhibition. This study developed a highly efficient selection method for protease inhibitory mAbs by coexpressing 3 recombinant proteins in the periplasmic space of *Escherichia coli*—an antibody clone, a protease of interest, and a β-lactamase modified by insertion of a protease cleavable peptide sequence. During functional selection, inhibitory antibodies prevent the protease from cleaving the modified β-lactamase, thereby allowing the cell to survive in the presence of ampicillin. Using this method to select from synthetic human antibody libraries, we isolated panels of mAbs inhibiting 5 targets of 4 main protease classes: matrix metalloproteinases (MMP-14, a predominant target in metastasis; MMP-9, in neuropathic pain), β-secretase 1 (BACE-1, an aspartic protease in Alzheimer's disease), cathepsin B (a cysteine protease in cancer), and Alp2 (a serine protease in aspergillosis). Notably, 37 of 41 identified binders were inhibitory. Isolated mAb inhibitors exhibited nanomolar potency, exclusive selectivity, excellent proteolytic stability, and desired biological functions. Particularly, anti-Alp2 Fab A4A1 had a binding affinity of 11 nM and inhibition potency of 14 nM, anti-BACE1 IgG B2B2 reduced amyloid beta ($A\beta_{40}$) production by 80% in cellular assays, and IgG L13 inhibited MMP-9 but not MP-2/-12/-14 and significantly relieved neuropathic pain development in mice.

protease inhibitor | monoclonal antibody | functional selection | MMP | BACE-1

Proteases regulate important physiological processes and are involved in essential pathogenesis of viruses, and therefore represent attractive targets for pharmaceutical development (1, 2). Human genome contains 569 proteases of 68 families (3), belonging to 5 main classes based on their catalytic mechanisms: aspartic, cysteine, threonine, serine, and metalloproteases. Existing in a delicate balance of networks with their endogenous inhibitors and substrates, proteases maintain the body's homeostasis. Dysregulation of proteolysis, however, causes a variety of diseases ranging from cancer, inflammation, and cardiovascular disorders to osteoporosis, neuropathic pain, and degenerative diseases (4–9). Notably, it has been estimated that proteases account for 5 to 10% of all drug targets being studied for therapeutic development (10). Numerous protease inhibitors are currently on the market for the treatment of coagulation, hypertension, viral infection, cancer, and diabetes through targeting well-established proteases such as angiotensin-converting enzyme and HIV proteases (10). Nevertheless, small-molecule inhibitors are often limited by lack of specificity and/or appropriate pharmacokinetic properties required for effective and safe protease-based therapy (11). These challenges are well reflected by failed clinical trials of historical attempts to inhibit matrix metalloproteinases (MMPs) as a cancer therapy (12, 13), and more recent ones to inhibit β-secretase 1 (BACE-1) for the remediation of Alzheimer's disease (14). Consequently, despite decades of intensive efforts, conventional drug discovery strategies have only achieved a limited success by targeting a tiny fraction of all therapeutically relevant proteases.

Biologics, for example, monoclonal antibodies (mAbs), provide exquisite specificity capable of distinguishing between closely related protease family members (15–21). Their stability in serum, potential to cross blood–brain barrier, novel design as prodrugs, and improved effector functions offer significant advantages over small-molecule therapeutics (22–24). In addition to pharmaceutical applications, specific inhibitory mAbs targeting individual proteases of biomedical importance are highly valuable as research tools to characterize protease degradomes. Since the invention of mAb technology in 1975, tremendous progress has been made in mAb discovery and engineering that forms the core of the biopharmaceutical industry today. However, current mAb selection/screening methods, including hybridoma, phage panning, single-cell PCR, cell surface display coupled flow cytometry, and so forth, are primarily based on binding affinities but not inhibitory function. Potentially important inhibitory clones that have weak binding affinities can be lost during the repeated cycles of competitive binding. As a result, there is a high level of probability that few or none of the selected binders are inhibitory (25). Furthermore, generated mAbs often exhibit suboptimal inhibition properties and are vulnerable to being cleaved by the protease target (26). Aiming to facilitate the direct identification of protease inhibitory mAbs with desired pharmacological properties, we developed a functional selection method, built on our experience with periplasmic coexpression of Ab fragments and active human proteases (27). To demonstrate the feasibility and generality of our method, we selected 5 drug targets representing 4 protease classes.

Significance

Proteases precisely control a wide variety of physiological processes and thus are important drug targets. Compared with small-molecule inhibitors, monoclonal antibodies (mAbs) are attractive, as they provide required specificity. However, finding inhibitory mAbs is often a bottleneck, largely due to lack of a function-based selection method. We overcame this obstacle and successfully isolated mAbs that effectively inhibited 5 therapeutic targets spanning 4 basic classes of proteases. Our mAb inhibitors are highly selective and deliver desired biochemical and biological actions, including reduction of amyloid beta formation in vitro and pain relief in animal behavioral tests. Thus, the technique described here can be readily applied to many pathophysiologically important proteases for the discovery and engineering of therapeutic mAbs.

Author contributions: T.L. and X.G. designed research; T.L., Z.M., C.C., K.B.L., A.R., C.B., and X.L. performed research; T.L., Z.M., C.C., K.B.L., X.L., R.-R.J., and X.G. analyzed data; X.G. supervised the project; and T.L., R.-R.J., and X.G. wrote the paper.

The authors declare no conflict of interest.

This article is a PNAS Direct Submission.

[1]To whom correspondence may be addressed. Email: xge@engr.UCR.edu.

This article contains supporting information online at www.pnas.org/lookup/suppl/doi:10.1073/pnas.1903330116/-/DCSupplemental.

Results

Design of Functional Selection for Protease Inhibitory mAbs. To select mAbs that inhibit proteases, 3 recombinant proteins—a clone from an antibody library, the protease of interest, and the protease substrate acting as an in vivo sensor—must be produced in the same location. We hypothesize that *Escherichia coli* periplasmic coexpression is ideal for this task because the oxidative environment and associated molecular chaperons facilitate disulfide formation needed to produce antibody fragments and many human proteases in their active form. In addition, large combinatorial libraries have been routinely constructed in *E. coli* thanks to its high transformation efficiency. The crucial aspect of this method is a cellular protease inhibition sensor; our design is to engineer β-lactamase TEM-1, a periplasmic hydrolase of β-lactam antibiotics, by inserting a protease-specific cleavable peptide sequence. When the modified TEM-1 is cleaved by the protease of interest, it loses its β-lactam hydrolytic activity, and thus the cell cannot grow in the presence of ampicillin. Conversely, when proteolytic activity of the target is blocked by a coexpressed antibody, TEM-1 is spared to confer ampicillin resistance to the host cell. Therefore, this live or die selection can identify antibody clones that specifically inhibit the activity of the targeted protease (Fig. 1*A*).

To demonstrate the generality of this functional selection method, we chose 5 disease-associated targets from 4 major classes of proteases: MMP-9 (neuropathic pain) (28), MMP-14 (metastasis) (29), aspartic protease BACE1 (Alzheimer's disease) (30), serine protease Alp2 of *Aspergillus fumigatus* (aspergillosis) (31), and cysteine protease cathepsin B (cancer and neurodegenerative disorders) (32). The extracellular/catalytic domains (cd) of these targets without their propeptide sequences were cloned downstream of a pLac promoter and a pelB leader for periplasmic expression. Enzymatic assays showed that produced proteases were functional with expected activities (*SI Appendix*, Fig. S1). Yields of 0.5 to 2.0 mg of active soluble proteases per liter of culture were typically achieved (except BACE1, which yielded 0.1 μg per liter culture), suggesting the feasibility of their inhibition by coexpressed Fabs, which are usually produced at similar level in periplasm (27).

Distinct Selection Windows for Protease Inhibitors. To select inhibitory mAbs with high potencies, protease-specific substrates with relatively fast kinetics (k_{cat}/K_ms) were used for TEM-1 insertion sequence design. Synthetic peptide substrates RLPLGI, SGRIGFLRTA, and KLHFSKQ were chosen for cdMMP-9, cdMMP-14, and cathepsin B, respectively. For BACE1, a peptide sequence EISEVKMDAEY was derived from its physiological substrate amyloid precursor protein (APP). As the physiological substrate of Alp2 is unknown, for its TEM-1 design, we chose a generic serine protease substrate sequence KLRSSKQ, which can be efficiently cleaved by Alp2 in vitro (*SI Appendix*, Fig. S1). Flanked by flexible serine–glycine linkers at both ends, that is, GSG–peptide–SGG, these cleavable peptide sequences were introduced between Gly196 and Glu197 of TEM-1 (*SI Appendix*, Fig. S2). This site is located on an exposed surface loop away from the β-lactamase active center and has been exploited for the construction of cellular sensors (33, 34). Survival curves of *E. coli* cells expressing modified TEM-1s without carrying genes of associated proteases were measured on agar plates supplemented with 0 to 1,000 μg/mL ampicillin. Results showed that the minimal inhibitory concentrations (MICs) were 500 μg/mL or higher (Fig. 1*B* and *SI Appendix*, Fig. S3), suggesting that peptide insertion did not significantly disrupt TEM-1 catalytic function,

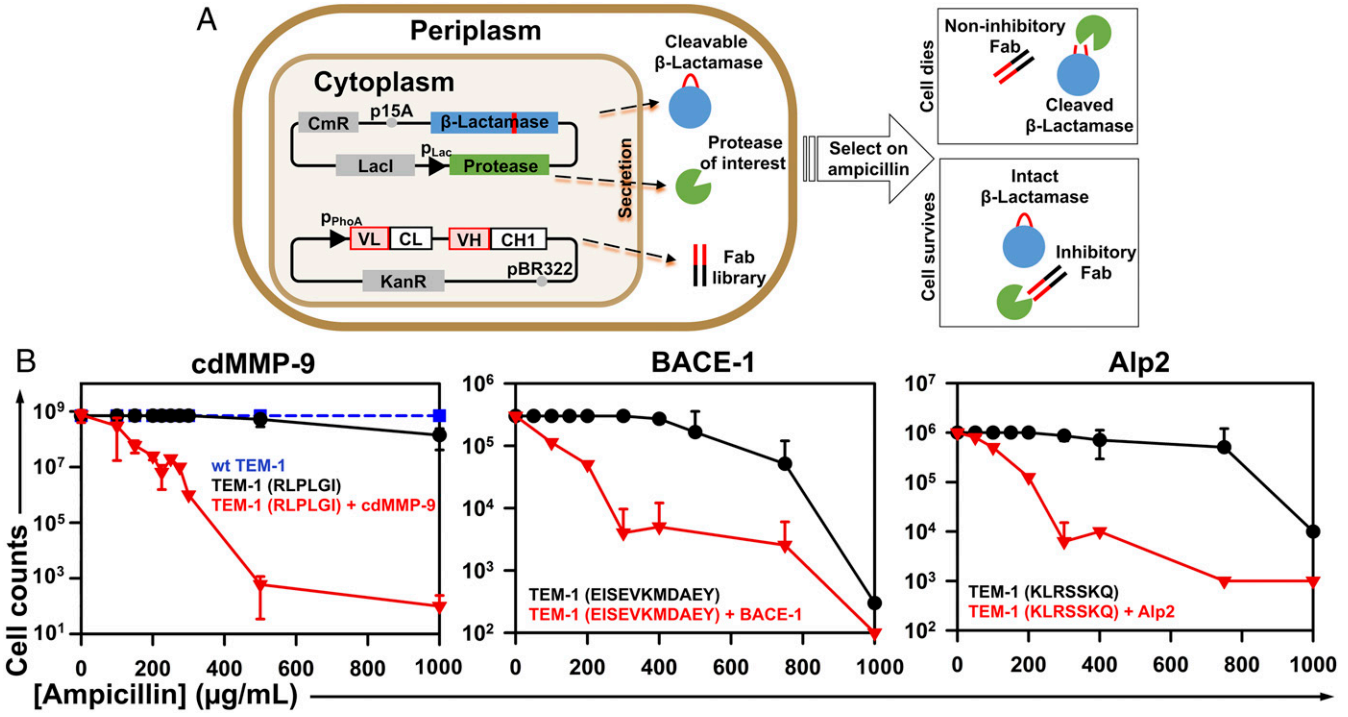

Fig. 1. Functional selection design for protease inhibitory antibodies. (*A*) Scheme showing that 3 recombinant proteins are simultaneously coexpressed in the periplasmic space of *E. coil*—a clone from the Fab library, the protease of interest, and the modified β-lactamase TEM-1 with a cleavable peptide insertion. The protease extracellular/cd under a lac promoter and TEM-1 under its native promoter are cloned into a low copy number (p15A ori) plasmid of chloramphenicol resistance (CmR). The antibody Fab library under a phoA promoter is cloned into a medium copy number (pBR322 ori) plasmid carrying kanamycin resistance (KanR). If the Fab has no inhibition, the protease will cleave TEM-1 leading to cell death in the presence of ampicillin. An inhibitory Fab blocks proteolytic activity which allows TEM-1 to remain intact, resulting in cell growth on ampicillin plates. (*B*) Selection windows for cdMMP-9 (*Left*), BACE-1 (*Middle*), and Alp2 (*Right*) inhibitors. TEM-1 was modified by inserting the protease-specific cleavage peptide sequences (shown in parentheses) between Gly196 and Glu197 of TEM-1 (*SI Appendix*, Fig. S2). At 0 to 1,000 μg/mL ampicillin, survival curves of *E. coli* cells transformed with modified TEM-1s without protease genes were measured (black circles) and compared with those for cells coexpressing both modified TEM-1s and the associated proteases (red triangles). The survival curve with WT TEM-1 is shown as a blue dashed line. Experiments were repeated 3 times with 2×YT agar plates containing 0.1 mM IPTG.

although the activities of modified TEM-1s were less than that of wild-type (WT) TEM-1, especially at high ampicillin concentrations (Fig. 1*B*, dashed line). However, when the associated proteases were periplasmically coexpressed, the MICs dramatically decreased to 200 μg/mL or lower, indicating that proteolytic cleavages of modified TEM-1s resulted in loss of their β-lactamase activity. Overall, the significant disparity between the survival curves with (red triangles) and without (black circles) coexpressed proteases provided distinct windows for effective selection of inhibitors. To optimize selection conditions, protease expression level was also up- or down-regulated by adding isopropyl β-D-1-thiogalactopyranoside (IPTG) or glucose. With a relatively high yield and high catalytic activity, the leakage expression of cdMMP-14 in the presence of 2% glucose was sufficient to effectively cleave the associated TEM-1-(SGRIGFLRTA) and resulted in an MIC of 150 μg/mL (*SI Appendix*, Fig. S3). As too much protease activity would result in the selection of inhibitors with high potency or high expression, and thus reduce the diversity of isolated clones, keeping cdMMP-14 expression at low levels should be beneficial. Therefore, 200 μg/mL ampicillin with 2% glucose was determined as the condition for cdMMP-14 inhibitory antibody selection. In contrast, other tested protease targets exhibited low expression levels and/or low activities, and thus overexpression is favorable to boost protease production. Therefore, 300 μg/mL ampicillin with 0.1 mM IPTG was applied for these proteases (*SI Appendix*, Table S1). Overall, these conditions yielded a 100% survival rate in the absence of protease and nearly complete cell death in the presence of protease, with the survival rates 2 to 3 orders of magnitudes lower.

Isolation of Multiple Potent mAb Inhibitors for Each Protease. To promote generation of inhibitory mAbs targeting protease reaction clefts (21), a human Fab synthetic library of 1.1×10^9 diversity encoding CDR-H3s with 23 to 27 amino acids was constructed downstream of a phoA promoter and an STII leader (Fig. 1*A*). Obtained Fab library plasmids were transformed to *E. coli* competent cells bearing the reporter plasmids for each protease. Libraries of 1.5 to 8.6×10^8 diversity were generated and subjected to functional selection for each protease inhibition under predetermined conditions (*SI Appendix*, Table S1). Surviving colonies were then individually screened by culturing in liquid media under more stringent conditions, that is, by increasing ampicillin concentration by 100 μg/mL. Taking anti-cdMMP-14 as an example, 190 clones survived after the initial selection, and the secondary screening narrowed them down to 161. Among them, 40 were randomly picked for DNA sequencing, and 38 unique Fabs were identified. Applying similar procedures, 5 to 20 monoclonal Fabs were successfully discovered for each of the other tested proteases (*SI Appendix*, Table S1).

Three to 8 Fabs from each selection experiment (total 41) were produced for biochemical characterizations (Table 1). Binding affinity measurements by biolayer interferometry and ELISA confirmed that all of the tested Fabs bound to their protease targets with dissociation constants (K_Ds) ranging from less than 10 nM to more than 1 μM (*SI Appendix*, Fig. S4). Among the tested 41 Fabs, 20 of them had K_D values < 250 nM. Particularly, anti-MMP9 Fab H4, anti-BACE1 Fab B3B12, anti-Alp2 Fab A4A1, and anti-cathepsin B Fab CBA3 exhibited a K_D of 6.9, 10, 11, and 16 nM, respectively. Inhibitory functions of purified Fabs were assayed with associated proteases and their fluorescence resonance energy transfer (FRET) peptide substrates. Results indicated that 37 out of 41 tested Fabs were inhibitors (*SI Appendix*, Fig. S5), equivalent to a 90% overall success rate, that is, the ratio of inhibitors over binders. Among these noninhibitors, 2 anti-MMP9 and 2 anti-Alp2 Fabs did not prevent their target proteases from cleaving the peptide substrates. Among isolated inhibitory Fabs, 57% of them (21 Fabs) showed potent inhibition with calculated inhibition constant (K_I) values < 250 nM (Table 1). Particularly, Fabs H4, B3B12, A4A1, and CBA3 had a K_I of 57, 26, 14, and 91 nM, respectively. Converting 2 anti-MMP9 and 2 anti-BACE1 inhibitory Fabs of nanomolar potencies into their IgG format improved their affinities and potencies as expected; for example, B3B12 IgG exhibited K_D of 7.2 nM and K_I of 16 nM (Table 1). Rapid isolation of multiple potent inhibitory mAbs

Table 1. Isolated inhibitory antibodies toward 4 classes of proteases

Type	Target	Peptide insert	Fab*	CDR-H3 (length)	K_D (nM)†	K_I (nM)†
Metallo-	MMP-9 (neuropathic pain)	RLPLGI	H4	SSLAWAQDRVYKPVEAMTWAYGMDY (25)	6.9	57
			H3	RFEPGLLKRNKRWISYTLCEAGYGMDY (27)	98 (71)‡	71 (52)‡
			L13	KYMVFGTRMGWVEHTDFAGQGYYAMDY (27)	120 (53)‡	160 (120)‡
			H25	CKLYTSYMIPVGSDSVNRCMSSYGMDY (27)	450	300
	MMP-14 (cancer)	SGRIGFLRTA	2B4	SDSAVYSVRRMGSSGLAAYAMDY (23)	66	95
			2B12	DCCSCVFSQSAGITLACVYVMDY (23)	76	130
			1A5	LDFLMRDIYYDLGGGALGWLIKYAMDY (27)	57	160
			2B10	QLFACWRQSILTPPLLSAMMMGYAMDY (27)	46	220
			2D9	GVTRFTNDASVGQVWAGAYGMDY (23)	260	240
			2A6	VVRMLPVRCIPRCIKTTLPLYGMDY (25)	130	440
Aspartic	BACE-1 (Alzheimer's)	EISEVKMDAEY	B3B12	YICGHRWRDFDMWRARTGVNYAMDY (25)	10 (7.2)‡	26 (16)‡
			B1A4	HYYVSVGSGIDY (12)	20 (16)‡	41 (37)‡
			B2B5	WHGYPPGYSYYSSFSSSGFDY (21)	130	80
			B2B2	YWGYYAWFGSHPWAYGAFDY (20)	52	85
			B2B3	SASGIDY (7)	100	110
			B2B9	SSSSYYYGMDY (11)	110	120
			B2B6	DNSICVLTQKEVDTKFLVGQHSYVMDY (27)	28	130
			B1B3	ERSSCPVGWRDSRFGADGYGLEY (23)	31	210
Serine	Alp2 (aspergillosis)	KLRSSKQ	A4A1	FGSWSYAIDY (10)	11	14
			A4A2	KTSDQYLLVGGSFFKLRDCCYVMDY (25)	110	220
			A4A7	GRSPGPYAVCGNLFRSVSYGMDY (23)	420	300
Cysteine	cathepsin B (cancer)	KLHFSKQ	CBA3	GFAWSPGLDY (10)	16	91
			CBA2	YGYPGGYHFWGWWSSPYAFDY (21)	200	120
			CBA1	GGGSWSAMDY (10)	300	210

*Only Fabs with inhibition constants (K_Is) < 500 nM are shown. Clones are ranked by their K_I values.
†See statistical analysis of K_D and K_I in *SI Appendix*, Table S2.
‡Data of associated IgGs are shown in parentheses.

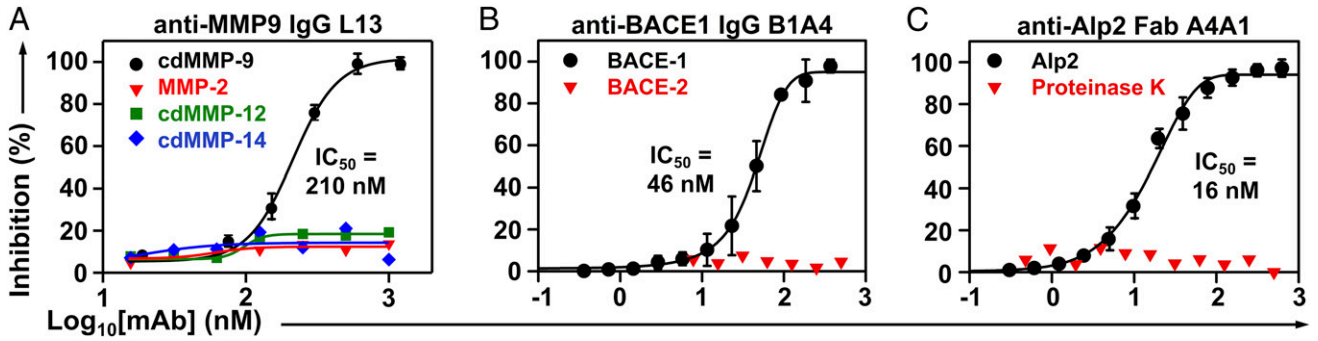

Fig. 2. Inhibition potency and selectivity. (*A*) Anti-MMP9 IgG L13, (*B*) anti-BACE1 IgG B1B4, and (*C*) anti-Alp2 Fab A4A1. Inhibition assays were measured using FRET peptide substrates.

targeting all 5 tested proteases from $>10^8$ library clones demonstrated the effectiveness and robustness of this selection system.

Inhibitory mAbs Are Highly Selective, Functional on Physiological Substrates, and Proteolytically Stable. Inhibition selectivity of 11 representative mAbs was tested. As results in Fig. 2*A* and *SI Appendix*, Fig. S5 show, IgGs H3 and L13 inhibited cdMMP-9 with K_Is of 52 and 120 nM, respectively, but did not inhibit structurally conserved (cd)MMP-2/-12/-14 (56 to 59% sequence similarity over cdMMP-14), even at 1 μM. Fabs 2B4, 2B12, and 1A5 inhibited cdMMP-14 with K_Is of 95 to 160 nM but did not inhibit cdMMP-9 at 500 nM (*SI Appendix*, Fig. S5). Similarly, IgGs B3B12 and B1A4 inhibited BACE-1 with nanomolar potency (K_I = 16 and 37 nM, respectively) but not BACE-2 (Fig. 2*B* and *SI Appendix*, Fig. S5) with its cd sharing 70% sequence with BACE-1; Fab A4A1 inhibited Alp2 (K_I = 14 nM) but not proteinase K, a broad-spectrum serine protease (Fig. 2*C*); and Fabs CBA3, CBA2, and CBA1 inhibited cathepsin B completely but not cathepsin K at the same Fab concentrations (*SI Appendix*, Fig. S5). Next, anti-cdMMP-9, anti-Alp2, and anti-BACE1 mAbs were exanimated for their inhibitory functions on the associated physiological/macromolecular substrates. Under tested conditions, Fab L13 reduced the degradation of type I collagen by cdMMP-9 from 61 to 4% (Fig. 3*A*), Fab A4A1 reduced the hydrolysis of FITC-conjugated collagen by Alp2 from 90 to 38% (Fig. 3*C*), and IgG B1A4 reduced cleavage of $APP_{571–696}$ by BACE-1 from 86 to 37% (*SI Appendix*, Fig. S6). Furthermore, in in vitro assays using HEK293 cells expressing APP, IgG B2B2 reduced amyloid beta ($A\beta_{40}$) production 80% in a dose-dependent manner with an apparent IC_{50} of 330 nM (Fig. 3*B*). To test proteolytic stability of inhibitory antibodies with target proteases in vitro, 1 μM purified Fabs were incubated with 1 μM respective protease at 37 °C. Sodium dodecyl sulfate polyacrylamide gel electrophoresis (SDS/PAGE) revealed that, after exposure to equal molar of the protease for 24 h, Fabs L13, 2B4, and A4A1 remained 93%, 76%, and 95% intact (Fig. 4).

Identification of Active Site and Exosite Inhibitors. To understand the inhibition mechanism, we measured cdMMP-9 kinetics in the presence of various concentrations of its inhibitory mAbs. When concentration of Fab L13 increased from 0 to 250 nM, the Lineweaver–Burk plots of cdMMP-9 indicated an unaltered maximum velocity V_{max} and increased Michaelis constant K_m, suggesting that Fab L13 performed as a competitive inhibitor (Fig. 5*A*). In contrast, with increasing concentrations of Fab H4, the kinetics of cdMMP-9 showed decreases on both V_{max} and K_m values, suggesting an uncompetitive inhibition mode. In addition, ELISA of Fab L13 on immobilized cdMMP-9 with the presence of nTIMP-2, an endogenous inhibitor of MMP-9 recognizing its reaction cleft (35), revealed that high concentrations of nTIMP-2 displaced L13 on binding to cdMMP-9 (Fig. 5*B*). However, nTIMP-2 did not interfere with H4 on its binding to cdMMP-9 in a similar competitive ELISA. These results suggest that L13 had its epitope overlapping with that nTIMP-2, while H4 did not share any epitope with nTIMP-2. Collectively, Fab L13 is an active site competitive inhibitor, and Fab H4 is an exosite uncompetitive inhibitor presumably delivering its blockage function by an allosteric mechanism.

Anti-MMP9 IgG L13 Exhibits Neuropathic Pain Attenuation Efficacy In Vivo. As MMP-9 is required in the early phase of neuropathic pain development after nerve injury (28), we further evaluated the pain relief efficacy of MMP-9 inhibitory IgG L13 in paclitaxel (PTX)-induced neuropathic pain in mice. PTX evoked robust mechanical allodynia, a cardinal feature of neuropathic pain, by decreasing paw withdrawal threshold (Fig. 6*A*) and increasing paw withdrawal frequency to a subthreshold filament (0.6 g; Fig. 6*B*).

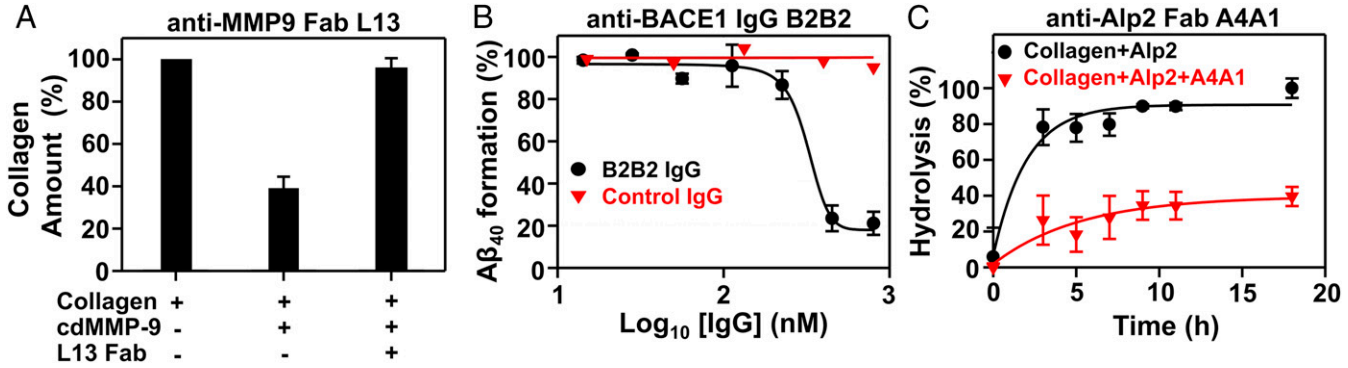

Fig. 3. Inhibitory functions of isolated mAbs on proteolysis of physiological/macromolecular substrates. (*A*) Fab L13 blocked MMP-9 from hydrolyzing type I collagen. (*B*) Inhibition of $A\beta_{40}$ formation by IgG B2B2 in cellular assays. HEK293F cell cultures expressing $APP_{571–696}$ were incubated with IgG for 72 h. Generated $A\beta_{40}$ was measured by ELISA. (*C*) Fab A4A1 blocked Alp2 from hydrolyzing FITC-conjugated type I collagen.

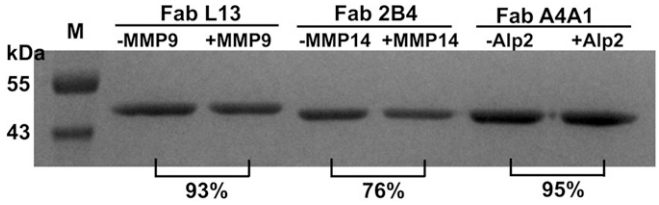

Fig. 4. In vitro proteolytic stability with target proteases. SDS/PAGE of 1 μM Fabs after incubation with 1 μM of the target protease for 12 h. The relative amounts of remaining Fabs were determined by densitometric analysis.

In contrast to polyclonal human control IgG which did not change the animals' behavioral responses, intrathecal injection of 200 μg of IgG L13, given 15 d after the first PTX administration, significantly increased the withdrawal threshold and reduced the withdrawal frequency ($P < 0.001$, 2-way ANOVA) (Fig. 6).

Discussion

In this study, we chose 5 disease-associated proteases representing 4 basic classes with diverse catalytic chemistries and surface topologies (*SI Appendix*, Fig. S7). More specifically, while MMPs and cathepsins display well-pronounced catalytic clefts and BACE-1 shows a large reaction cavity, the active site of Alp2 is relatively small and shallow. Interestingly, when 2 synthetic Fab libraries carrying CDR-H3s of 23 to 27 or 5 to 21 amino acids were separately applied for BACE-1 (*SI Appendix*, Table S1), we were able to isolate inhibitory mAbs from both libraries. Among 8 potent anti-BACE1 inhibitors, 5 of them carry long CDR-H3s (>20 aa), and the remaining 3 have short CDR-H3s (7 to 12 aa) (Table 1). However, when these 2 synthetic Fab libraries were combined and jointly applied for Alp2, the most potent Fab isolated (A4A1 with a K_I of 14 nM) was derived from the short CDR-H3 library. These results suggest that, at least for active site inhibitors, appropriate CDR-H3 length distribution could be a considerable factor to accommodate desired paratope conformations that are compatible with targeted protease topology.

Our functional selection achieved an exceptionally high success rate of 90%, that is, 37 out of 41 tested binders were inhibitors. We further analyzed these 4 noninhibitory clones, to reason how they could survive during this live or die selection. Anti-MMP9 Fabs H44 and L6 exhibited binding affinities of 520 ± 130 nM and 230 ± 95 nM, respectively, but did not inhibit cdMMP-9 from cleaving its FRET peptide substrate. To define their epitopes, we conducted competitive ELISA on immobilized cdMMP-9 in the presence of nTIMP-2. Results showed that high concentrations of nTIMP-2 displaced Fabs on binding to cdMMP-9 (*SI Appendix*, Fig. S8), indicating that H44 and L6 Fabs had their epitopes at least partially overlapping with that of nTIMP-2, and thus could block the access of macromolecular substrates such as TEM-1(RLPLGI) that allowed cell survival during the selection. Unfortunately, similar competitive ELISA cannot be carried out for anti-Alp2 because Alp2 macromolecular inhibitors are not available. Interestingly, however, 2 noninhibitory anti-Alp2 Fabs were isolated with a peptide insertion KLRSSKQ which was derived from a generic substrate of serine proteases. Notably, the survival rates of *E. coli* cells coexpressing Alp2 and TEM-1(KLRSSKQ) gradually decreases, then plateaus when ampicillin concentration increases (Fig. 1 *B*, *Right*). This suboptimal survival curve implies the chance that noninhibitory clones are able to escape from the ampicillin selection. Therefore, the outcomes of noninhibitory clones could be potentially remedied by applying insertion peptide sequences with high cleaving efficiency and/or performing additional rounds of selection with more stringent conditions.

Other than antibody library and peptide insertion sequence designs, the selection conditions, such as concentrations of ampicillin and inducer, culture media, and temperature, can be customized for each protease target, allowing rapid downsizing of libraries. Our selection resulted in numerous clones after the secondary screening (e.g., 161 anti-MMP14 and 73 anti-BACE1), of which only small subsets were randomly picked for full characterizations, due to time constrain. Therefore, it is likely that additional inhibitory mAbs could be identified from the remaining uncharacterized pools. Among tested mAbs, more than half of identified inhibitors had a potency $K_I < 250$ nM, while some showed a weaker potency ($K_I > 1$ μM). Considering that all these mAbs were isolated from synthetic libraries, ranges of different affinity/potency were expected. Interestingly, we also found that highly potent anti-BACE1 B3B12 and B1A4 were produced at low yields with 0.1 mg or less purified Fabs per liter of culture, while low-potency B2B5 and B2B2 Fabs were generated at higher yield, with 0.56 and 1.3 mg per liter of culture (*SI Appendix*, Table S3). Presumably, these weak inhibitors were isolated because of their high titers which can compensate for their low potency. In addition, our approach of periplasmic coexpression facilitates the disulfide formation required for activities of many human proteases; for example, cds of BACE1 and cathepsin B have 3 and 6 disulfide bonds, respectively. Furthermore, proteases were produced in their propeptide-free form; thus isolated mAbs can directly inhibit the activated proteases. Certain macromolecular inhibitors of proteases, especially the canonical mechanism inhibitors including endogenous inhibitors and inhibitory mAbs, tend to be slowly cleaved by the targeted protease (36). However, the mAbs isolated in this study exhibited excellent proteolytic stability (Fig. 4). It is likely that this benefited from the nature of in vivo selection, because inhibitory function and thus the integrity of Fabs must be maintained over the entire course for cell survival.

In summary, this study described a high-throughput method for selecting protease inhibitory mAbs. Compared with recent technology developments such as epitope synthetic mimicry (37), convex paratope design (21), competitive phage elution (16), cytoplasmic genetic selection (38), and epitope-specific fluorescence-activated cell sorter (39), this method directly relies on functional inhibition and offers the following advantages: 1) an exceptionally high successful rate as the ratio of inhibitors over binders (*SI Appendix*, Table S1); 2) exclusive selectivity against proteases of the same family (Fig. 2 and *SI Appendix*, Fig. S5); 3) relatively high proteolytic resistance to the target proteases (Fig. 4); 4) both

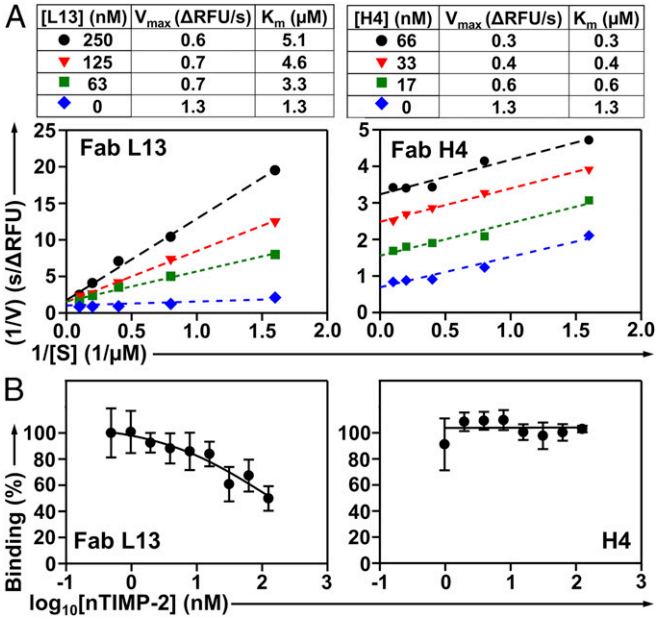

Fig. 5. Inhibition mechanisms of anti-MMP9 Fabs. (*A*) Lineweaver–Burk plots of cdMMP-9 in the presence of 62.5, 250, and 500 nM Fab L13 (*Left*) or 66, 33, and 16.5 nM Fab H4 (*Right*). (*B*) Competitive ELISA of Fab L13 (*Left*) or Fab H4 (*Right*) on immobilized cdMMP-9 in the presence of 1 to 125 nM nTIMP-2.

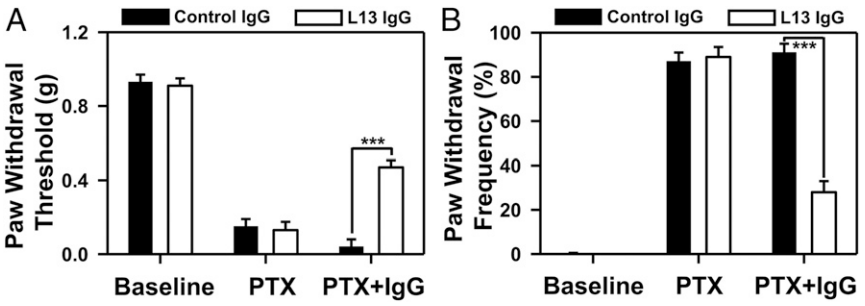

Fig. 6. Analgesic effects of MMP-9 inhibitor IgG L13 in neuropathic pain induced by the chemotherapy agent paclitaxel (PTX) in male mice; 200 ng IgG L13 was intravenously administered on day 15 after PTX injections. Behavioral tests of neuropathic pain symptom mechanical allodynia, evaluated by paw withdrawal threshold (*A*) and frequency (*B*), were performed in a blinded manner ($n = 7$ mice for control IgG, and $n = 6$ mice for L13 IgG). ***$P < 0.001$, 2-way ANOVA with Tukey's post hoc test.

active-site and allosteric inhibitors can be identified (Fig. 5); and 5) multiple inhibitory mAbs are available for providing a rich pool for lead candidate characterization and optimization (Table 1). Considering that 2% of the human genome encode proteases and half of them are extracellular and thus targetable by mAbs, the method developed here can be readily applied for the discovery of mAbs that are able to inhibit many therapeutically important proteases. Notably, lanadelumab, a plasma kallikrein (pKal) inhibitor, was approved by the Food and Drug Administration in 2018 as the first protease inhibitory mAb for treating hereditary angioedema. As numerous BACE-1 compound inhibitors failed in clinical trials, we sincerely hope our technique can promote mAb discovery for protease inhibitors. In addition to mAbs, other biologics, especially endogenous inhibitors of proteases, can be engineered using the similar approach.

Materials and Methods

Protease cleavable peptide sequences with flanking serine–glycine linkers were assembled by using synthetic oligonucleotides and cloned between G196 and E197 of TEM-1 to generate modified TEM-1 genes. Reporter plasmids for periplasmic coexpression of proteases of interest and associated modified TEM-1s were constructed and tested for β-lactamase activities on agar plates containing 0 to 1,000 μg/mL ampicillin. Synthetic human Fab libraries were transformed to cells harboring reporter plasmids and subjected to inhibitory selection under predetermined conditions for each protease. Fabs and IgGs of isolated antibody clones were produced and biochemically characterized by biolayer interferometry, ELISA, and inhibition assays using FRET peptides and macromolecular substrates. Biological functions of anti-MMP9 IgG L13 were also tested with neuropathic pain mouse model. All animal experiments were approved by the Institutional Animal Care and Use Committees (IACUC) of Duke University. Detailed experimental procedures are provided in *SI Appendix, SI Materials and Methods*.

ACKNOWLEDGMENTS. This work was supported by National Institutes of Health Grants R01GM115672 (to X.G.) and R01DE17794 (to R.-R.J.), and National Science Foundation CAREER 1453645 (to X.G.).

1. B. Turk, D. Turk, V. Turk, Protease signalling: The cutting edge. *EMBO J.* **31**, 1630–1643 (2012).
2. E. Deu, M. Verdoes, M. Bogyo, New approaches for dissecting protease functions to improve probe development and drug discovery. *Nat. Struct. Mol. Biol.* **19**, 9–16 (2012).
3. C. López-Otín, J. S. Bond, Proteases: Multifunctional enzymes in life and disease. *J. Biol. Chem.* **283**, 30433–30437 (2008).
4. C. López-Otín, L. M. Matrisian, Emerging roles of proteases in tumour suppression. *Nat. Rev. Cancer* **7**, 800–808 (2007).
5. I. Prassas, A. Eissa, G. Poda, E. P. Diamandis, Unleashing the therapeutic potential of human kallikrein-related serine proteases. *Nat. Rev. Drug Discov.* **14**, 183–202 (2015).
6. R. B. Singh, S. P. Dandekar, V. Elimban, S. K. Gupta, N. S. Dhalla, Role of proteases in the pathophysiology of cardiac disease. *Mol. Cell. Biochem.* **263**, 241–256 (2004).
7. L. Troeberg, H. Nagase, Proteases involved in cartilage matrix degradation in osteoarthritis. *Biochim. Biophys. Acta* **1824**, 133–145 (2012).
8. R. R. Ji, Z. Z. Xu, X. Wang, E. H. Lo, Matrix metalloprotease regulation of neuropathic pain. *Trends Pharmacol. Sci.* **30**, 336–340 (2009).
9. B. De Strooper, Proteases and proteolysis in Alzheimer disease: A multifactorial view on the disease process. *Physiol. Rev.* **90**, 465–494 (2010).
10. M. Drag, G. S. Salvesen, Emerging principles in protease-based drug discovery. *Nat. Rev. Drug Discov.* **9**, 690–701 (2010).
11. B. Turk, Targeting proteases: Successes, failures and future prospects. *Nat. Rev. Drug Discov.* **5**, 785–799 (2006).
12. C. M. Overall, O. Kleifeld, Towards third generation matrix metalloproteinase inhibitors for cancer therapy. *Br. J. Cancer* **94**, 941–946 (2006).
13. R. E. Vandenbroucke, C. Libert, Is there new hope for therapeutic matrix metalloproteinase inhibition? *Nat. Rev. Drug Discov.* **13**, 904–927 (2014).
14. R. Vassar, BACE1 inhibitor drugs in clinical trials for Alzheimer's disease. *Alzheimers Res. Ther.* **6**, 89 (2014).
15. Y. Wu *et al.*, Structural insight into distinct mechanisms of protease inhibition by antibodies. *Proc. Natl. Acad. Sci. U.S.A.* **104**, 19784–19789 (2007).
16. L. Devy *et al.*, Selective inhibition of matrix metalloproteinase-14 blocks tumor growth, invasion, and angiogenesis. *Cancer Res.* **69**, 1517–1526 (2009).
17. J. K. Atwal *et al.*, A therapeutic antibody targeting BACE1 inhibits amyloid-β production in vivo. *Sci. Transl. Med.* **3**, 84ra43 (2011).
18. E. L. Schneider *et al.*, A reverse binding motif that contributes to specific protease inhibition by antibodies. *J. Mol. Biol.* **415**, 699–715 (2012).
19. J. A. Kenniston *et al.*, Inhibition of plasma kallikrein by a highly specific active site blocking antibody. *J. Biol. Chem.* **289**, 23596–23608 (2014).
20. T. David *et al.*, Factor XIa-specific IgG and a reversal agent to probe factor XI function in thrombosis and hemostasis. *Sci. Transl. Med.* **8**, 353ra112 (2016).
21. D. H. Nam, C. Rodriguez, A. G. Remacle, A. Y. Strongin, X. Ge, Active-site MMP-selective antibody inhibitors discovered from convex paratope synthetic libraries. *Proc. Natl. Acad. Sci. U.S.A.* **113**, 14970–14975 (2016).
22. Y. J. Yu *et al.*, Therapeutic bispecific antibodies cross the blood-brain barrier in nonhuman primates. *Sci. Transl. Med.* **6**, 261ra154 (2014).
23. S. K. Sharma, K. D. Bagshawe, Antibody directed enzyme prodrug therapy (ADEPT): Trials and tribulations. *Adv. Drug Deliv. Rev.* **118**, 2–7 (2017).
24. X. Wang, M. Mathieu, R. J. Brezski, IgG Fc engineering to modulate antibody effector functions. *Protein Cell* **9**, 63–73 (2018).
25. J. Zhang *et al.*, Identification of inhibitory scFv antibodies targeting fibroblast activation protein utilizing phage display functional screens. *FASEB J.* **27**, 581–589 (2013).
26. K. B. Lee, Z. Dunn, X. Ge, Reducing proteolytic liability of a MMP-14 inhibitory antibody by site-saturation mutagenesis. *Protein Sci.* **28**, 643–653 (2019).
27. D. H. Nam, X. Ge, Direct production of functional matrix metalloproteinase–14 without refolding or activation and its application for in vitro inhibition assays. *Biotechnol. Bioeng.* **113**, 717–723 (2016).
28. Y. Kawasaki *et al.*, Distinct roles of matrix metalloproteases in the early- and late-phase development of neuropathic pain. *Nat. Med.* **14**, 331–336 (2008).
29. Y. Itoh, M. Seiki, MT1-MMP: A potent modifier of pericellular microenvironment. *J. Cell. Physiol.* **206**, 1–8 (2006).
30. R. Vassar, D. M. Kovacs, R. Yan, P. C. Wong, The β-secretase enzyme BACE in health and Alzheimer's disease: Regulation, cell biology, function, and therapeutic potential. *J. Neurosci.* **29**, 12787–12794 (2009).
31. A. Abad *et al.*, What makes *Aspergillus fumigatus* a successful pathogen? Genes and molecules involved in invasive aspergillosis. *Rev. Iberoam. Micol.* **27**, 155–182 (2010).
32. C. S. Gondi, J. S. Rao, Cathepsin B as a cancer target. *Expert Opin. Ther. Targets* **17**, 281–291 (2013).
33. A. Galarneau, M. Primeau, L. E. Trudeau, S. W. Michnick, Beta-lactamase protein fragment complementation assays as in vivo and in vitro sensors of protein protein interactions. *Nat. Biotechnol.* **20**, 619–622 (2002).
34. J. R. Porter, C. I. Stains, D. J. Segal, I. Ghosh, Split β-lactamase sensor for the sequence-specific detection of DNA methylation. *Anal. Chem.* **79**, 6702–6708 (2007).
35. C. Fernandez-Catalan *et al.*, Crystal structure of the complex formed by the membrane type 1-matrix metalloproteinase with the tissue inhibitor of metalloproteinases-2, the soluble progelatinase A receptor. *EMBO J.* **17**, 5238–5248 (1998).
36. C. J. Farady, C. S. Craik, Mechanisms of macromolecular protease inhibitors. *ChemBioChem* **11**, 2341–2346 (2010).
37. N. Sela-Passwell *et al.*, Antibodies targeting the catalytic zinc complex of activated matrix metalloproteinases show therapeutic potential. *Nat. Med.* **18**, 143–147 (2011).
38. M. Gal-Tanamy *et al.*, HCV NS3 serine protease-neutralizing single-chain antibodies isolated by a novel genetic screen. *J. Mol. Biol.* **347**, 991–1003 (2005).
39. T. Lopez *et al.*, Epitope-specific affinity maturation improved stability of potent protease inhibitory antibodies. *Biotechnol. Bioeng.* **115**, 2673–2682 (2018).

Supplementary Information for

Functional Selection of Protease Inhibitory Antibodies

Tyler Lopez[a], Zahid Mustafa[a], Chuan Chen[a], Ki Baek Lee[a], Aaron Ramirez[a], Chris Benitez[a], Xin Luo[b], Ru-Rong Ji[b], Xin Ge[a1]

[a]Department of Chemical and Environmental Engineering, University of California, Riverside, CA 92521; [b]Center for Translational Pain Medicine, Department of Anesthesiology, Duke University Medical Center, Durham, NC 27710

[1]To whom correspondence may be addressed: xge@engr.ucr.edu

CONTENT:

www.pnas.org/cgi/doi/10.1073/pnas.1903330116

SI Materials and Methods

Development of protease cleavage reporters. Plasmid carrying β-lactamase TEM-1 gene was PCR amplified to introduce unique *Xba*I and *Nco*I recognition sites between G196 and E197 of TEM-1. The PCR product was ligated with 5' phosphorylated oligonucleotide assembled adapters encoding protease specific cleavable peptide sequences (**Table S1**) flanked by serine-glycine linkers (GSG[peptide]SGG) to obtain genes of modified TEM-1s. Genes encoding extracellular or catalytic domains of human MMP-9 (residue 107-443 without fibronectin domains), human MMP-14 (residue 114-320), human β-secretase 1 (BACE1, residue 46-457), *Aspergillus fumigatus* autophagic serine protease 2 (Alp2, residue 136-495), and human cathepsin B (residue 66-339) without their associated propeptide sequences were PCR assembled and cloned into *Sfi*I sites on pMopac16 carrying a p15A origin and a pelB leader peptide to obtain their periplasmic expression plasmids (1). The modified TEM-1 genes were then sub-cloned into these protease expression plasmids using *Nsi*I and *Nhe*I sites to generate reporter plasmids (**Fig 1A**). From these reporter plasmids, protease genes were then removed by PCR amplifying the TEM-1 gene regions followed by self-ligation to obtain plasmids carrying modified TEM-1 genes without protease genes. All cloned plasmids were confirmed by DNA sequencing. β-lactam ring hydrolysis activities of modified TEM-1s in the absence or presence of associated proteases were tested by culturing transformed *E. coli* BL21 cells on 2×YT agar plates containing 34 μg/mL chloramphenicol, 50 μg/mL kanamycin, 0-0.1 mM IPTG, 0-2% glucose, and 0-1000 μg/mL ampicillin at 30 ºC for 16 hours. Colony numbers were determined by serial dilutions and survival curves were plotted to identify the optimal conditions of inhibitor selection for each protease target.

Selection of protease inhibitory antibodies. Fab library genes containing regular (2) or ultra-long CDR-H3s (3) were PCR amplified and cloned into pHPK (kanR, pBR322 ori, phoA promoter, and STII leader). Constructed library plasmids pHPK-Fab were transformed into *E. coli* Jude-I electrocompetent cells for amplification. Randomly picked colonies were sequenced for library quality and diversity tests. Electrocompetent cells of BL21 harboring the reporter plasmid for individual protease were transformed with 100 μg library pHPK-Fab. Transformed cells were cultured on 2×YT agar plates of pre-determined selection conditions specific for each protease (**Table S1**). Small aliquots of transformed cells were also serially diluted and cultured on 2×YT agar plates supplemented with 34 μg/mL chloramphenicol and 50 μg/mL kanamycin for library size determination. Colonies surviving the initial selection were individually inoculated in the 2×YT selection media with a higher ampicillin concentration for secondary screening. Well-grown clones were selected for Fab plasmid extraction and V_H and V_L DNA sequencing.

Production of antibodies and proteases. Genes of isolated Fabs were sub-cloned and transformed into BL21 cells for periplasmic production by culturing in 2×YT media at 30 ºC for 12 hours. Fabs with a hexahistidine tag at the C-terminal of V_H were purified using Ni-NTA agarose (Qiagen) from periplasmic fractions prepared by lysozyme and osmotic shock (4). Associated IgGs were produced in HEK293F (ThermoFisher Scientific) as previously described (5). Purified Fabs and IgGs were dialyzed at 4 ºC against the following assay buffers: 50 mM Tris-HCl pH 7.5, 150 mM NaCl, 5 mM $CaCl_2$, 0.4 mM $ZnCl_2$ for cdMMP-9; 50 mM Tris-HCl pH 7.5, 150 mM NaCl, 5 mM $CaCl_2$, 0.1 mM $ZnCl_2$ for cdMMP-14; PBS pH 7.5 for Alp2 and cathepsin B; and 20 mM HEPES, 125 mM NaCl pH 5.0 for BACE-1. Dialyzed antibody samples were concentrated by 10 kDa MWCO ultrafiltration (Amicon), and their purity and concentration were determined by SDS-PAGE and UV spectrophotometer (BioTek). C-terminal hexahistidine tagged cdMMP-9, cdMMP-12, cdMMP-14, Alp2, cathepsin B, and cathepsin K were produced in their active format in the periplasmic space of *E. coli* without refolding or activation (1) and purified using Ni-NTA agarose (Qiagen). MMP-2 was purchased from AnaSpec Inc. BACE1-Fc fusion was produced by HEK293F using pcDNA-intron-SPL-BACE1-Fc-WPRE containing human IgG1 heavy chain with the associated signal peptides and Woodchuck hepatitis virus posttranscriptional regulatory elements to enhance the expression. Cultured media was clarified by centrifugation and 0.45 μm filtration, and BACE1-Fc was purified by protein A affinity chromatography (GenScript).

Biochemical characterizations of isolated antibodies. Binding kinetics of produced antibodies towards associated protease targets were analyzed by using biolayer interferometry (ForteBio). For Fabs, biotinylated proteases were immobilized on streptavidin biosensors, and Fab binding to the sensors in absence of protease was monitored as backgrounds. For IgGs, protein A sensors were used and protease bindings without IgG were checked as backgrounds. k_{on} and k_{off} were determined for K_D calculations. Competitive ELISA of Fabs on immobilized cdMMP-9/-14 in the presence of 1 nM-1 μM nTIMP-2 was also tested. Fab *in vitro* stability was tested by incubating 1 μM Fab with 1 μM of the respective protease in the assay buffer for 12 hours and the samples were analyzed by SDS-PAGE.

For inhibition tests, 1 μM Fabs were 2-fold serially diluted into protease specific assay buffer and incubated with 1-10 nM proteases for 30 min at room temperature. The kinetic measurements were started with the addition of 1 μM following FRET peptide substrates: M-2350 (Mca-KPLGL-Dpa(Dnp)-AK-NH_2, Bachem) for MMP-9/14, M-2420 (Mca-SEVNLDAEFK(Dnp)-OH, Bachem) for BACE-1, Mca-KLRSSKQK(Dnp) (Biomatik) for Alp2, and M-2595 (Abz-GIVRAK(Dnp)-OH, Bachem) for cathepsin B. The generated fluorescence signals were monitored with excitation and emission wavelengths at 325 and 392 nm (except M-2595 at 320/420 nm) using a fluorescence plate reader (BioTek). Inhibition percentages at given concentrations were calculated by comparing the initial reaction rates in the presence or absence of inhibitor. IC_{50} was determined as the concentration that achieved 50% inhibition, and K_I values were calculated using $K_I = IC_{50}/(S/K_m+1)$. V_{max} and K_m at various Fab concentrations were measured to determine the inhibition type. FRET inhibition assays were also used for selectivity tests of isolated Fabs with the relevant proteases.

For inhibition tests on macromolecular substrates, 1 μM cdMMP-9 was incubated with 300 μg/mL rat collagen I (Corning) with or without 1 μM Fab L13 in MMP-9 assay buffer at 37 ºC for 24 h. Samples were taken hourly and analyzed by SDS-PAGE under non-reducing conditions. For amyloid precursor protein (APP) degradation studies, $APP_{571-696}$ was cloned to the C-terminal of maltose binding protein (MBP) for *E. coli* expression and purified using amylose resin (NEB). 5 μM purified MBP-APP was incubated with 1 μM BACE1-Fc in the absence or presence of 1 μM IgG in BACE-1 assay buffer at 37 ºC for 24 h. In addition, $APP_{571-696}$ was cloned to a pcDNA plasmid carrying a SPE leader for secretion expression. Transfected HEK293F cells were cultured in Expi293 media for 72 hrs with the presence of 14-800 nM purified IgG. The supernatants were clarified by centrifugation and 0.45 μm filtration and produced $A\beta_{1-40}$ was quantified by ELISA (Abcam). For Alp2, 10 μg/mL FITC-conjugated type I collagen (AnaSpec) was incubated with 2 μM Alp2 in PBS at room temperature in the presence or absence of 10 μM Fab for 18 h. The reaction solution was centrifuged at 3,000 g for 10 min and the fluorescence of the supernatant was measured at Ex/Em=490/520 nm.

Biological functions of anti-MMP9 IgG L13: Neuropathic pain measurement. Wild-type CD1 mice (male and female, 8-10 wks, Charles River Laboratories) were housed at Duke vivarium animal facility, and all animal experiment protocols were approved. To produce chemotherapy-associated neuropathic pain, paclitaxel (PTX, 2 mg/kg, i.p.) was injected at day 0, 2, 4, and 6 (6). Intrathecal injection was performed as described previously (7), mice were anesthetized with isoflurane and a spinal cord puncture was performed between the L5 and L6 level to deliver drugs (10 μL) using a 30G needle. All behavioral tests were performed in boxes on an elevated metal mesh floor under stable room temperature and humidity. Mice were habituated to the environment for at least 2 days before the experiments. To assess mechanical allodynia, the plantar surface of the left hind-paw was stimulated using a series of von Frey fibers with logarithmically increasing stiffness (0.02-2.56 gram, Stoelting), presented perpendicularly to the central plantar surface. 50% paw withdrawal threshold was determined following Dixon's up-down method. The frequency response was measured by stimulating the hind-paw with a 0.4 gram von Frey hair for ten times and the percentage withdrawal response was calculated as frequency. All the behavioral tests were performed in a blinded manner.

SI References

1. Nam DH, Ge X. Direct production of functional matrix metalloproteinase--14 without refolding or activation and its application for in vitro inhibition assays. *Biotechnol Bioeng.* **113**, 717–723 (2016).
2. Persson H, et al. CDR-H3 Diversity is not Required for Antigen Recognition by Synthetic Antibodies. *J Mol Biol.* **425**, 803–811 (2013).
3. Nam DH, Ge X. Generation of Highly Selective MMP Antibody Inhibitors. *Methods Mol Biol.* **1731**, 307–324 (2018).
4. Rodriguez C, Nam DH, Kruchowy E, Ge X. Efficient Antibody Assembly in *E. coli* Periplasm by Disulfide Bond Folding Factor Co-expression and Culture Optimization. *Appl Biochem Biotechnol.* **183**, 520–529 (2017).
5. Chen KE, et al. Use of a Novel Camelid-Inspired Human Antibody Demonstrates the Importance of MMP-14 to Cancer Stem Cell Function in the Metastatic Process. *Oncotarget.* **9**, 29431–29444 (2018).
6. Chen G, Park CK, Xie RG, Ji RR. Intrathecal Bone Marrow Stromal Cells Inhibit Neuropathic Pain via TGF-β Secretion. *J Clin Invest.* **125**, 3226–3240 (2015).
7. Xu ZZ, et al. Inhibition of Mechanical Allodynia in Neuropathic Pain by TLR5-mediated A-fiber Blockade. *Nat Med.* **21**, 1326–1331 (2015).

Table S1. Conditions and results of selections for protease inhibitory antibodies

Protease	**cdMMP-9**		**cdMMP-14**	**BACE1**		**Alp2**	**cathepsin B**
Peptide insert	RLPLGI	SGRIGFLRTA	SGRIGFLRTA	EISEVKMDAEY		KLRSSKQ	KLHFSKQ
Library							
CDR-H3 length (aa)	23, 25, 27	23, 25, 27	23, 25, 27	23, 25, 27	5-21	5-21, 23, 25, 27	5-21
Size	6.2×10^8	4.1×10^8	8.6×10^8	7.1×10^8	1.8×10^8	2.9×10^8 *	1.5×10^8
Initial selection							
[Amp] (μg/mL)	300	300	200	300	300	300	300
[IPTG] (mM)	0.1	0.1	0	0.1	0.1	0.1	0.1
[glucose] (%)	0	0	2	0	0	0	0
Temp (°C)	30	30	30	30	30	30	30
# of clones remaining	22	37	190	24	87	43	122
Secondary screening							
[Amp] (μg/mL)	400	400	300	400	400	500	400
[IPTG] (mM)	0.1	0.1	0	0.1	0.1	0.1	0.1
[glucose] (%)	0	0	0	0	0	0	0
Temp (°C)	30	30	30	30	30	30	30
# of clones remaining	13	15	161	21	52	29	7 †
Sequenced	13	7	40	8	5	10	7
Unique correct sequences	13	7	38	6	5	8	5
Fabs produced	8	5	6	6	5	8	3
Binders	8	5	6	6	5	8	3
Inhibitors	8	3	6	6	5	6	3

Note:

* Long CDR library (CDR-H3 length = 23, 25 or 27) and normal CDR library (CDR-H3 length = 5-21) were combined for selection.

† Only 10 clones were randomly picked for the secondary screening.

Table S2. Statistical analysis for inhibitory antibodies shown in Table 1

Target	Fab	Binding affinity *			Inhibition potency †				
		k_{on} ± S.E. (1/Ms)	k_{off} ± S.E. (1/s)	K_D ± S.E. (nM)	a ± S.E.	b ± S.E.	I_0 ± S.E.	IC_{50} ± S.E. (nM)	K_I ± S.E. (nM)
MMP-9	H4	$(4.62\pm0.42)\times10^{6}$	$(3.18\pm0.26)\times10^{-2}$	6.9±1.2	94.22±0.26	49.90±0.51	98.78±0.66	101.4±1.0	57.3±0.6
	H3	$(4.91\pm0.18)\times10^{4}$	$(4.83\pm0.13)\times10^{-3}$	98±6.2	89.81±0.51	61.31±1.38	119.85±1.65	125.9±2.6	71.2±1.5
	L13	$(8.30\pm0.11)\times10^{4}$	$(1.00\pm0.014)\times10^{-2}$	121±3.3	90.67±0.53	119.56±3.26	265.96±4.51	276.7±6.4	156.4±3.6
	H25	$(6.89\pm0.16)\times10^{4}$	$(3.11\pm0.038)\times10^{-2}$	450±16	90.76±0.43	277.45±5.21	513.42±6.85	538±10.2	304.1±5.8
MMP-14	2B4	$(1.24\pm0.19)\times10^{4}$	$(7.88\pm0.56)\times10^{-4}$	66±15	85.35±0.62	49.65±1.46	97.51±1.96	105.0±3.1	94.5±2.7
	2B12	$(7.03\pm0.18)\times10^{4}$	$(5.27\pm0.25)\times10^{-3}$	76±5.6	93.79±0.49	57.50±1.13	135.94±1.60	139.3±2.3	125.3±2.1
	1A5	$(4.35\pm0.087)\times10^{4}$	$(2.47\pm0.13)\times10^{-3}$	57±4.1	91.70±0.37	83.49±1.19	169.35±1.70	175.9±2.5	158.3±2.3
	2B10	$(4.01\pm0.29)\times10^{4}$	$(1.85\pm0.097)\times10^{-3}$	46±5.8	88.32±0.38	107.69±2.14	236.76±2.74	249.2±4.1	224.3±3.6
	2D9	$(1.51\pm0.30)\times10^{4}$	$(3.87\pm0.16)\times10^{-3}$	256±62	93.06±0.31	103.57±1.50	258.04±1.88	264.8±2.7	238.3±2.5
	2A6	$(2.36\pm0.21)\times10^{4}$	$(3.02\pm0.11)\times10^{-3}$	128±16	92.22±0.47	199.55±3.73	477.07±4.92	491.7±7.4	442.6±6.7
BACE-1	B3B12	$(6.71\pm0.60)\times10^{5}$	$(6.83\pm0.37)\times10^{-3}$	10±1.5	93.73±0.40	12.70±0.23	31.47±0.29	32.2±0.4	25.6±0.3
	B1A4	$(4.20\pm0.34)\times10^{5}$	$(8.55\pm0.71)\times10^{-3}$	20±3.3	90.69±0.63	25.59±0.82	49.69±0.99	52.0±1.5	41.4±1.2
	B2B5	$(1.80\pm0.23)\times10^{5}$	$(2.42\pm0.27)\times10^{-2}$	134±32	98.08±0.30	32.08±0.40	99.64±0.55	100.2±0.8	79.8±0.6
	B2B2	$(1.77\pm0.18)\times10^{5}$	$(9.10\pm0.19)\times10^{-3}$	52±6.4	95.15±0.13	28.64±0.20	104.88±0.27	106.1±0.4	84.5±0.3
	B2B3	$(9.31\pm1.70)\times10^{4}$	$(9.70\pm0.23)\times10^{-3}$	104±22	96.44±0.59	73.81±1.63	138.00±2.16	140.4±3.2	111.7±2.5
	B2B9	$(1.80\pm0.35)\times10^{5}$	$(2.00\pm0.16)\times10^{-2}$	111±30	97.90±0.20	48.00±0.41	150.86±0.60	151.8±0.8	120.8±0.6
	B2B6	$(1.83\pm0.16)\times10^{5}$	$(5.12\pm0.13)\times10^{-3}$	28±3.1	100.16±0.10	58.19±0.22	157.75±0.33	157.7±0.4	125.5±0.4
	B1B3	$(4.16\pm0.88)\times10^{5}$	$(1.30\pm0.03)\times10^{-2}$	31±7.5	90.10±0.44	115.23±2.04	258.39±2.79	269.4±4.2	214.4±3.4
Alp2	A4A1	$(8.21\pm1.24)\times10^{4}$	$(8.66\pm0.62)\times10^{-4}$	10.5±2.3	93.32±0.53	6.13±0.17	15.44±0.25	15.8±0.3	14.0±0.3
	A4A2	$(8.21\pm0.42)\times10^{3}$	$(8.66\pm0.61)\times10^{-4}$	106±13	94.09±0.34	110.24±1.69	245.31±2.03	251.3±3.0	222.1±2.6
	A4A7	$(5.18\pm0.64)\times10^{3}$	$(2.19\pm0.11)\times10^{-3}$	420±74	85.10±0.52	140.39±3.20	319.04±4.12	340.6±6.7	301.0±5.9
cathepsin B	CBA3	$(4.82\pm0.26)\times10^{6}$	$(7.52\pm0.21)\times10^{-2}$	16±1.3	96.99±0.28	52.77±0.54	129.15±0.73	130.6±1.1	91.0±0.7
	CBA2	$(3.03\pm0.13)\times10^{5}$	$(5.90\pm0.13)\times10^{-2}$	195±13	81.71±0.37	67.08±1.50	162.59±1.74	175.9±2.8	122.6±2.0
	CBA1	$(2.10\pm0.13)\times10^{5}$	$(6.23\pm0.27)\times10^{-2}$	296±31	91.31±0.56	138.10±3.38	284.16±4.04	295.6±6.2	206.0±4.3

Note:

* Association (k_{on}) and dissociation (k_{off}) rates were measured at three Fab concentrations using biolayer interferometry. Averages of k_{on} and k_{off} and their standard errors (S.E.) were calculated with BLItz Pro software for determining dissociation constants K_D ± S.E. Obtained k_{on}, k_{off}, and K_D values are reported as two significant digits in **Table 1** and **Fig S4**.

† The correlations between inhibition percentage and Fab concentration were measured with 1 μM FRET peptide substrates. Using Sigma Plot, data fitting with the 3-parameter sigmoidal equation $y = a / (1+e^{-([I]-I_0)/b})$ generated a, b, I_0 parameters and their S.E. IC_{50} ± S.E. were then calculated for determination of inhibition constants (K_I ± S.E.) using equation $K_I = IC_{50}/(1+[S]/K_m)$, where [S] = 1μM and K_m is the Michaelis-Menten constant of tested protease (**Fig S1**). IC_{50} and K_I values are reported as two significant digits in **Table 1** and **Fig S5**.

Table S3. Yields of representative anti-BACE1 mAbs

mAb		Potency (nM)	Yield (mg/L)
Fab	B3B12	26	0.08
	B1A4	41	0.10
	B2B5	80	0.56
	B2B2	85	1.3
IgG	B3B12	16	2.0
	B1A4	37	2.0

Figure S1:

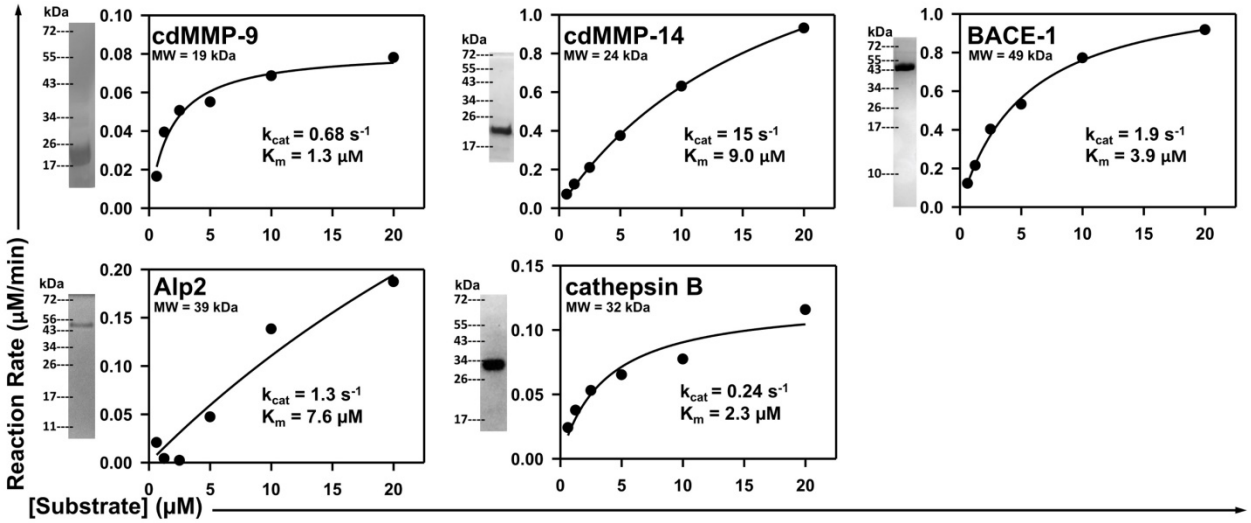

Fig. S1. Periplasmic production of extracellular / catalytic domains of human / fungal proteases in their active soluble format. Purified protases were analyzed by SDS-PAGE, and their enzymatic kinetics were measured with associated FRET peptide substrates.

Figure S2:

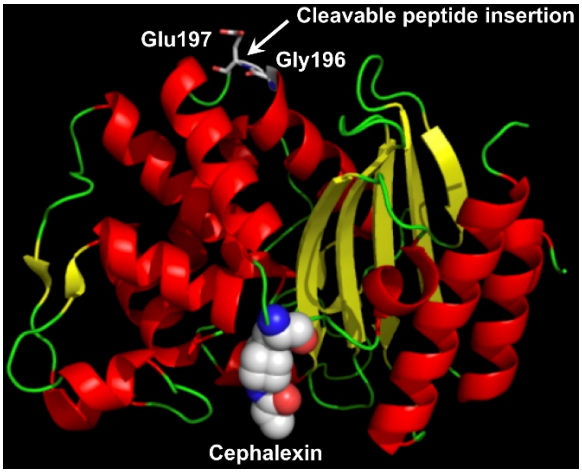

Fig. S2. Design of β-lactamase TEM1 sensor for protease inhibition. Structure (PBD, 4ZJ3) showing that the location of cleavage peptide insertion (between Gly196 and Glu197) is on a loop far away from the active site where inhibitors, e.g. cephalexin, bind. Images were generated by using PyMol.

Figure S3:

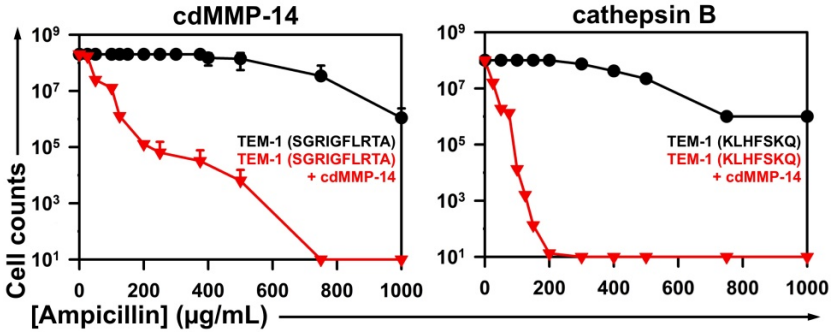

Fig. S3. Selection windows for cdMMP-14 and cathepsin B inhibitors. β-lactamase TEM-1 was modified by insertion of the protease specific cleavage peptide sequences (shown in parentheses) between Gly196 and Glu197 of TEM-1. At 0-1000 μg/mL ampicillin, survival curves of *E. coli* cells transformed with modified TEM-1s without protease genes were measured (black circles), and compared to those for cells co-expressing both modified TEM-1s and the associated proteases (red triangles). Experiments were repeated three times with 2×YT agar plates containing either 2% glucose for cdMMP-14 or 0.1 mM IPTG for cathepsin B.

Figure S4:

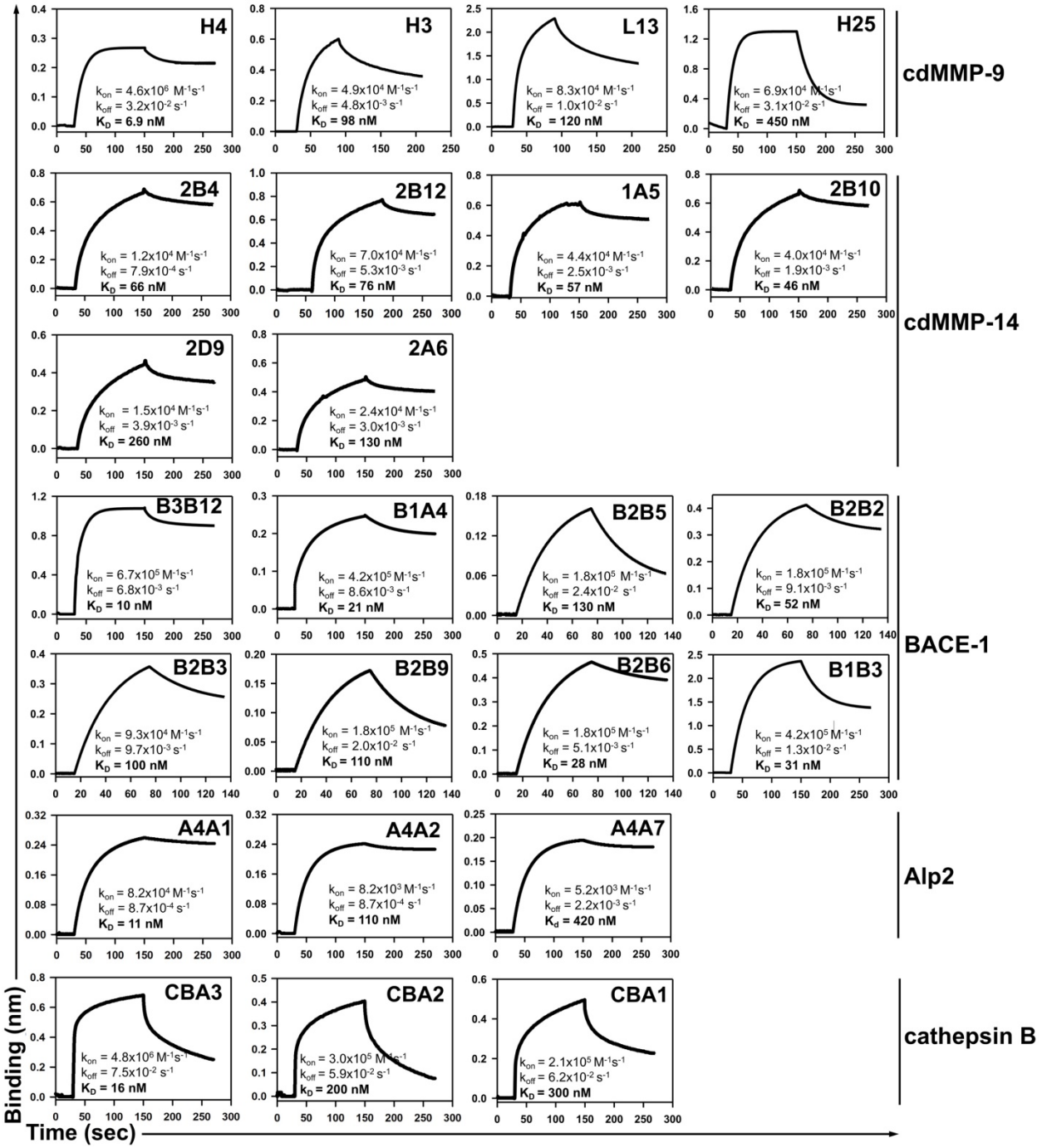

Fig. S4. **Binding kinetics of isolated Fabs to protease targets.** k_{on} and k_{off} values were measured by bio-layer interferometry and used for K_D calculation. Only Fab clones with K_I < 500 nM are shown in the same orders as in **Table 1**. See **Table S2** for statistical analysis.

Figure S5:

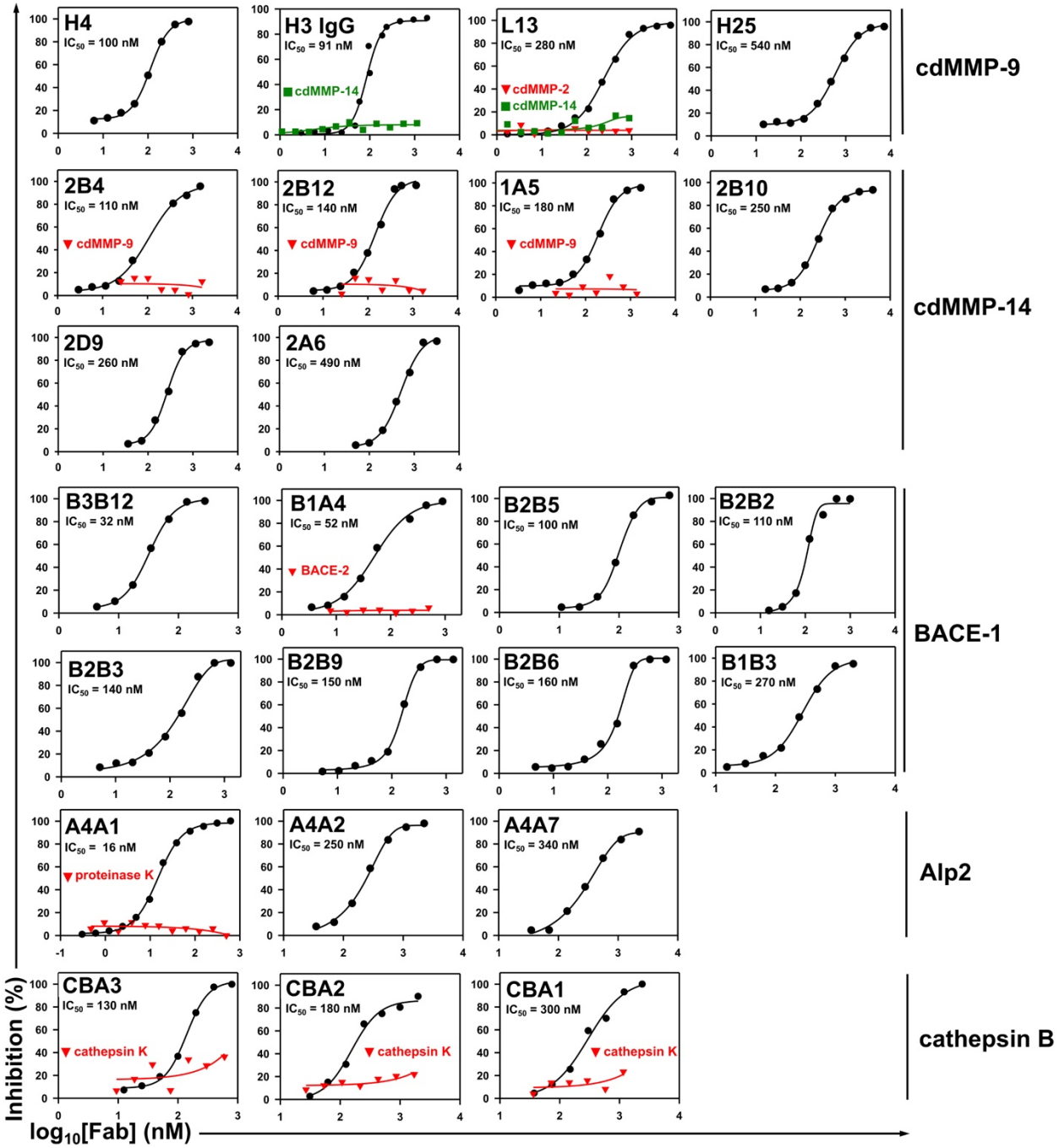

Fig. S5. Inhibition potencies of isolated Fabs. Inhibition IC_{50}s were measured by using FRET peptide substrates. Only Fab clones with K_I < 500 nM are shown in the same orders as in **Table 1**. Inhibition selectivity of representative Fabs was also tested. For anti-cdMMP9 clone H3, its IgG instead of Fab is shown. See **Table S2** for statistical analysis.

Figure S6:

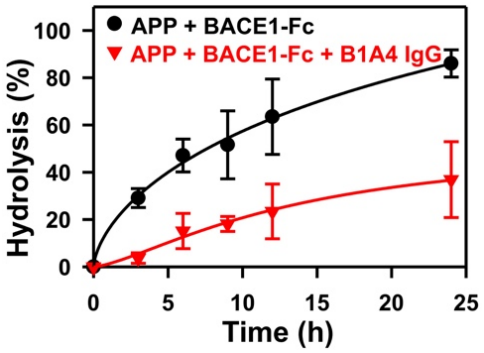

Fig. S6. Inhibitory functions of anti-BACE1 IgG B1A4 on proteolysis of amyloid precursor protein (APP). 5 μM MBP-APP was incubated with 1 μM BACE1-Fc in the absence or presence of 1 μM IgG B1B4 at 37 ^{o}C for 24 h. Samples were taken and analyzed by SDS-PAGE to quantify amounts of remaining APP. Purified BACE1-Fc exhibited catalytic kinetics k_{cat} of 0.23/min and K_m of 1.24 μM.

Figure S7:

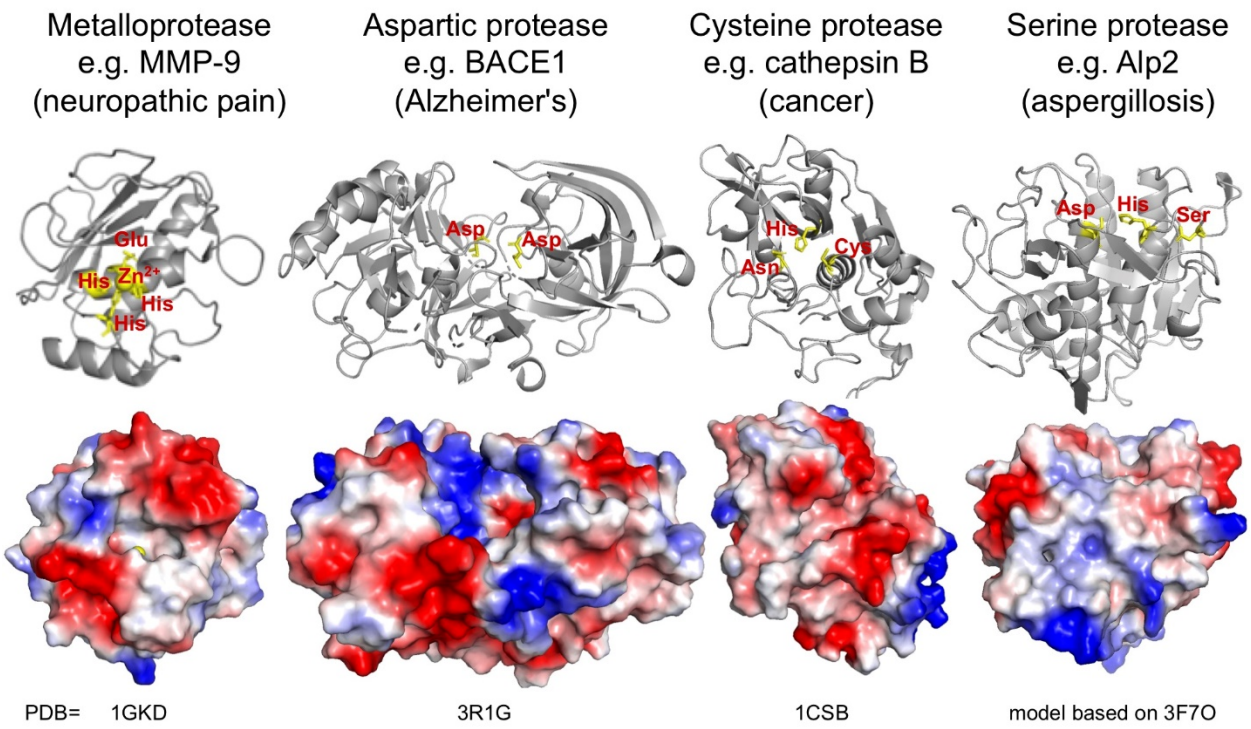

Fig. S7. Active sites and electrostatic surface potentials of representative proteases. Side chains of the catalytic residues are highlighted in yellow. Surface topologies display the reactive clefts or cavities of diverse conformation. Images were generated with indicated PDB files by using PyMol.

Figure S8:

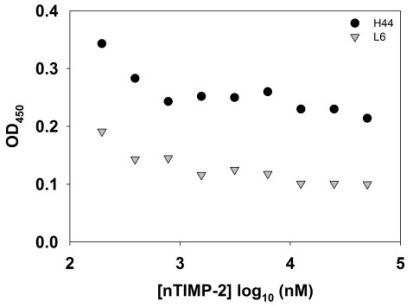

Fig. S8. Competitive ELISA of anti-MMP9 Fabs H44 and L6. 500 nM Fabs were incubated with 200 nM -50 μM nTIMP-2 for 15 min then added to wells coated with cdMMP-9. Captured Fabs were detected with anti-Fab-HRP.